2-2008

On Isoconcentration Surfaces of Three Dimensional Turing Patterns

Tilmann Glimm
Western Washington University, tilmann.glimm@wwu.edu

H. George E. Hentschel
Emory University

On isoconcentration surfaces of three dimensional Turing patterns ‡

Tilmann Glimm
Department of Mathematics, Western Washington University, Bellingham, WA 98225
H.G.E. Hentschel
Department of Physics, Emory University, Atlanta, GA 30322

Abstract. We consider three dimensional Turing patterns and their isoconcentration surfaces corresponding to the equilibrium concentration of the reaction kinetics. We call these surfaces *equilibrium concentration surfaces* (EC surfaces). They are the interfaces between the regions of "high" and "low" concentrations in Turing patterns. We give alternate characterizations of EC surfaces by means of two variational principles, one of them being that they are optimal for diffusive transport. Several examples of EC surfaces are considered. Remarkably, they are often very well approximated by certain minimal surfaces. We give a dynamical explanation for the emergence of Scherk's surface in certain cases, a structure that has been observed numerically previously in [De Wit *et al.*, 1997].

‡ This work was supported by NSF Grant No. IBN-0083653. We acknowledge support from the Center for Applied Mathematics and the Interdisciplinary center for the Study of Biocomplexity at the University of Notre Dame and the Biocomplexity Institute at Indiana University.
2000 Mathematics Subject Classification: 35K57, 74A50, 35A15, 92C15

1. Introduction

Since Turing first showed in the early 1950s that the interplay of diffusion and reactions of chemicals can give rise to self-organizing patterns of chemical concentrations in [Turing, 1952], there has been much interest in this pattern formation mechanism by both mathematicians and physicists. (See for instance [Murray, 2002] and references therein.) Experimentally, however, the Turing mechanism was first observed unambiguously in a chemical system in the early 1990s [Castets *et al.*, 1990, Ouyang and Swinney, 1991].

The basic idea of the Turing mechanism is that a homogeneous equilibrium concentration of the reaction kinetics can become unstable in the presence of diffusion, leading to heterogeneous distributions of the chemicals involved, which is somewhat surprising considering that diffusion normally smooths out concentration fluctuations. Many models of biological phenomena have been explained in terms of a Turing-type mechanism giving rise to the pattern observed in nature. Most prominent is probably the patterning of animals coats [Murray, 2002], but Turing-type mechanisms have also been used to explain the appearance of feather buds and fish skin [Shoji *et al.*, 2002]. Turing-type models for the emergence of skeletal patterns in embryonic vertebrate limb buds have also been proposed [Newman and Frisch, 1979], that have recently been supported by more biologically based reaction-diffusion models of limb skeletal patterning [Hentschel *et al.*, 2004, Miura and Maini, 2004, Izaguirre *et al.*, 2004].

It is noteworthy that although the general mathematical methodologies such as nonlinear stability analysis, bifurcation theory and singular perturbation theory are valid in any spatial dimension, most of the modeling work that has been done is two dimensional. Three-dimensional Turing patterns in a cube and their stability have, however, been studied with both periodic boundary conditions [Callahan and Knobloch, 1997, Callahan and Knobloch, 1999], as well as the more biologically plausible case of no-flux boundary conditions [Alber *et al.*, 2005].

In two dimensions, patterns can easily be visualized as density plots of the chemical concentrations. In three dimensions, one can correspondingly visualize patterns by means of a series of density plots of cross-sections, taken at regular height intervals, or by the lattice of local maxima and minima of concentration. Here we propose to study the *interfaces* between regions of high concentration and regions of low concentrations. More precisely, in Turing patterns, one can consider the isoconcentration surfaces corresponding to the equilibrium concentration of the Turing kinetics. In the following, we call these isoconcentration surfaces *equilibrium concentration surfaces*, or EC surfaces.

An interesting numerical study of three dimensional Turing patterns was conducted in [De Wit *et al.*, 1997], which found, among other structures, "twisted" lamellar structures in the Brusselator model. The EC surfaces in this "twisted" stationary Turing structure had a striking resemblance to Scherk's first surface, a minimal surface well-known in differential geometry. (For a brief reminder on minimal surfaces see Section 2

below.) Similar structures were recently also found numerically in the Gray-Scott model [Leppänen *et al.*, 2004]. [De Wit *et al.*, 1997] concluded that "in physicochemical systems driven out of equilibrium, our vision of 3D self-organization may be enriched by emphasizing isoconcentration surfaces, for which the salient variable is curvature, instead of the more traditional crystalline skeletal lattice of extrema of concentrations. These complementary and mutually supporting views open up a new path in the field of dissipative crystallography that should help in deciphering the experimental 3D textures."

In this paper, we aim to follow this suggestion and conduct an investigation of EC surfaces in three dimensional Turing patterns. We prove that they can be characterized by means of various variational principles. These principles are valid in two situations, namely they hold close to the equilibrium for general Turing patterns, and they hold far from equilibrium for a certain class of reaction kinetics. The most important of these principles states that EC surfaces are optimal for diffusive transport across the surface. We also give examples for EC surfaces of known Turing patterns. Interestingly, these EC surfaces are very close to minimal surfaces, an observation that was already implicit in [De Wit *et al.*, 1997]. Scherk's surface has been mentioned before, but in the other Turing patterns we consider, the EC surfaces are planes (sometimes with self-intersections), or periodic surfaces that approximates Schwarz' P-surface very closely, another well-known minimal surface. As a step towards a mathematical explanation of this interesting connection between EC surfaces and minimal surfaces, we use the variational principle for EC surfaces to derive a rough bound for the area difference between EC surfaces and minimal surfaces with the same boundary. Our assumptions are, however, very general, and so we found it hard to derive more conclusive information about the "closeness" of minimal surfaces and EC surfaces. We believe, however, that this is a promising avenue, and research should aim in the direction of which additional assumptions guarantee this "closeness."

We also anticipate that our results can be useful for the study of three dimensional biological structures, for example biological membranes [Meyer *et al.*, 1990], or skeletal patterns in Echinoidea, where periodic surfaces resembling for instance the Schwarz P-surface have been reported [Pawson and Donnay, 1969, Nissen, 1969]. It seems possible that these structures could be formed by a Turing mechanism. Indeed, in particular the result that these surfaces are optimal for diffusive transport is an interesting property in connection with the study of transport across membranes and its connection to their biological function. We also note that the optimal transport criterion is similar to other variational criteria concerning for example interfaces of two phase systems in material science. It has been shown for instance that certain periodic minimal surfaces are extremal for simultaneous transport of heat and electricity in two phase systems [Torquato *et al.*, 2002].

In order to be as self-contained as possible, we give a very brief reminder on the differential geometry of regular surfaces, and on minimal surfaces in particular, in Section 2. In Section 3, we briefly remind the reader of the Turing mechanism,

and then formulate and prove the variational principle for the EC surfaces. We give a "geometric" as well as a "chemical" formulation of the variational principles. In the first, one varies the shape of the surface, and keeps the chemical concentration constant; in the second, one varies the chemical concentration, albeit only allowing a certain subclass of perturbations. Based on this variational principle, we also derive a rough estimate for the area difference between an EC surface and minimal surfaces. In Section 4, we give a short overview of the EC surfaces in known three dimensional Turing patterns, partly based on the previous paper [Alber *et al.*, 2005], which treated the stability of Turing patterns in a the cube $[0, \pi]^3$. In the last Section, we finally aim to investigate the appearance and relative stability of the "Scherk-like" structure reported in[De Wit *et al.*, 1997]. Using linear stability analysis and Fourier analysis, we show how one can expect this structure to evolve from a certain class of initial conditions close to the equilibrium in a box $[0, 2\pi]^2 \times [-\alpha\pi, \alpha\pi]$, where α is a parameter. Our analysis yields that this emergence is best seen if α is approximately equal to the wave length of the Turing pattern.

2. The Geometry of Surfaces and Minimal Surfaces

In the following section, we give a brief reminder on the geometry of surfaces in $\mathbb{R}^3$ and on minimal surfaces in particular. We also state a useful formula for the mean curvature of level sets.

2.1. Regular surfaces

Let $S \subseteq \mathbb{R}^3$ be a regular surface in $\mathbb{R}^3$. This means that we have a domain $D \subseteq \mathbb{R}^2$ and a parametrization

$$\mathbf{X}\colon D \to S \subseteq \mathbb{R}^3, \quad (r, s) \mapsto \mathbf{X}(r, s),$$

which is of class at least C^2 and is a bijection onto S. The surface is regular if the Jacobian $D\mathbf{X}(r, s) = (\mathbf{X}_r\ \mathbf{X}_s)$ has full rank two at each $(r, s) \in D$. (Subscripts "r" and "s" denote differentiation here and in the following.)

At each point, the normal $\mathbf{N} = \mathbf{X}_r \times \mathbf{X}_s / |\mathbf{X}_r \times \mathbf{X}_s|$ is well defined and independent of the parametrization $\mathbf{X}$. (Here "$\times$" denotes the usual cross product in $\mathbb{R}^3$.) By definition, the tangent space T_xS to the surface S at x is perpendicular to $\mathbf{N}(x)$. Likewise, the tangent space $T_{\mathbf{N}(x)}S^2$ of S^2, the surface of the unit ball in $\mathbb{R}^3$, at the point $\mathbf{N}(x)$ is perpendicular to $\mathbf{N}(x)$. Thus the two tangent space are canonically isomorphic: $T_xS \simeq T_{\mathbf{N}(x)}S^2$. It follows that the differential $T\mathbf{N}_x\colon T_xS \to T_{\mathbf{N}(x)}S^2$ can be seen as an endomorphism of T_xS. With respect to the basis $\{\mathbf{X}_r, \mathbf{X}_s\}$, this mapping has the matrix $B = \{b_{ij}\}_{i,j=1,2}$, where the defining equations for the matrix elements are

$$\mathbf{N}_r = b_{11}\mathbf{X}_r + b_{12}\mathbf{X}_s$$
$$\mathbf{N}_s = b_{21}\mathbf{X}_r + b_{22}\mathbf{X}_s$$

The eigenvalues of B are usually denoted by κ_1 and κ_2 and called the *principal curvatures*. Other measures of local curvature are the following celebrated two quantities:

$$K = \det B = \kappa_1 \cdot \kappa_2 \quad \text{Gauss curvature}$$
$$H = \frac{1}{2}\text{Trace}\, B = \frac{1}{2}(\kappa_1 + \kappa_2) \quad \text{mean curvature}$$

We will be concerned mostly with the mean curvature of implicitly defined surfaces in the following. Recall that if $u(x, y, z)$ is a C^2 scalar function, and (x_0, y_0, z_0) is a point with $u(x_0, y_0, z_0) = 0$ and $|\nabla u(x_0, y_0, z_0)| \neq 0$, then there is a neighborhood Ω of (x_0, y_0, z_0) such that the equation $u(x, y, z) = 0$ defines a regular surface $S = \{(x, y, z) \colon u(x, y, z) = 0\}$ in Ω. Its normal at $(x, y, z) \in S$ is given by the normed gradient $\mathbf{N} = \nabla u/|\nabla u|$. One computes that the mean curvature is given by

$$H = \frac{1}{2}\text{div}\frac{\nabla u}{|\nabla u|} = \frac{1}{2|\nabla u|}\left(\nabla^2 u - \text{Hess}u[\mathbf{N}, \mathbf{N}]\right) \tag{1}$$

Here $\nabla^2 = \sum_i \partial_i^2$ is the Laplacian and $\text{Hess}u = \{\partial_{ij} u\}$ the Hessian.

Returning to the general theory of surfaces, the area element of S is given as $dS = |\mathbf{X}_r \times \mathbf{X}_s| dr\, ds$. So the integral of a function f over S is given by $\int_S f(x)\, dS = \int_D f(\mathbf{X}(r, s))|\mathbf{X}_r \times \mathbf{X}_s| dr\, ds$.

2.2. Minimal surfaces

The basic idea behind minimal surfaces is of course that these are those surfaces that minimize area. Traditionally, however, the term *minimal surface* has come to denote a slightly larger class of surfaces, namely those which are critical points (maxima, minima or saddle points) of the area functional $S \mapsto \int_S dS$. It is a classical result, dating back to Lagrange in 1760 and Meusnier in 1776, that these are precisely those surfaces for which the mean curvatures H vanishes everywhere.

The subject of minimal surfaces has been a subject of intense study for almost 250 years. In the 20th century, it was in particular Plateau's problem (i.e., the problem of finding a minimal surface which spans a given closed curve $\gamma \subseteq \mathbb{R}^3$) which has driven research in this area. In the last 20 years, the dramatic increase in computational power has opened a new world for scientific imaging and invigorated research on minimal surfaces. We will not make any attempt to summarize the vast literature here, but point to the many excellent textbooks on the subject, for example [Dierkes *et al.*, 1992], [Nitsche, 1989] and [Osserman, 1986].

Let us mention, however, that minimal surfaces can be found in nature in many different settings. Classically, of course, they can be realized as soap films on wire models (this is how Plateau studied them), and they have also been found as interfaces that separate the polymer types in block polymers. In the simplest case, a block copolymer consists of two polymer chains A and B. At low temperatures, the components separate into two domains to minimize the energetically unfavorable contacts between polymers

A and B. They cannot separate completely, however, because they are chemically bound. To minimize the contact, the interfaces must be (at least approximately) locally area-minimizing under the constraint of keeping the volumes on the two sides of the surface fixed. This problem is known as the isoperimetric problem and the corresponding surfaces have constant mean curvature. If the constant mean curvature is zero, they are minimal surfaces in the classical sense. For a brief, but very informative review article, see [Thomas, 1999]. [Hoffman, 1996] gives a short overview of the area with some critical remarks about its mathematical rigor. A good recent review article on the isoperimetric problem is [Ros, 2005].

3. Variational Principles for Equilibrium Concentration Surfaces of Turing Patterns

Here we state and prove variational principles for the surfaces of constant equilibrium concentration in three dimensional Turing patterns. These variational principles are valid in two situations: approximately for Turing patterns close to the Turing bifurcation, and exactly for a certain class of reaction kinetics. There are two similar formulations: A "geometric" formulation, where we fix the chemical field and vary the shape of the surface, and a "chemical formulation", where we consider variations of the chemical field. (A certain additional constraint is imposed on the admissible variations of the chemical field in this formulation.)

Let $\overline{u}(x)$, $x \in \Omega$, denote the chemical concentration for the Turing pattern in a three dimensional domain Ω. We denote the corresponding equilibrium concentration surface by $S_0 = \{x \in \Omega \colon \overline{u}(x) = u_0\}$, where u_0 is the equilibrium concentration of the reaction kinetics considered without the diffusion term. To formulate the variational principle, we consider local variations S of S_0. That is, we fix a closed curve γ on S_0 and consider surfaces S which are equal to S_0 outside of the domain bounded by γ, but which may differ from S_0 within this domain. We prove that for Dirichlet or Neumann (no-flux) boundary conditions on $\partial\Omega$, the surface S_0 maximizes the integral $\int_S \nabla\overline{u}(x) \cdot \mathbf{N} dS$ among all such surfaces S. Here $\mathbf{N}$ is the normal of S. (The orientation of $\mathbf{N}$ is chosen essentially such that the chemical concentration increases in the direction of $\mathbf{N}$, for more details see page 10.)

Note that the integral is just the diffusive flux of the chemical $\overline{u}$. So our result says that if we seek to maximize the diffusive flux through a surface, then we have to choose the EC surface S_0.

We also show in a related characterization that S_0 is a critical point of the functional $S \mapsto \int_S |\nabla\overline{u}(x)| dS$. Under certain conditions, we show that S_0 minimizes this functional, although for Dirichlet or Neumann conditions, it probably typically is a saddle point.

These previous variational principles are "geometric" in the sense that we considered variations of the surface shape for a fixed concentration function $\overline{u}(x)$. We also give a brief "chemical" formulation of the variational principle, where it is the chemical concentration which is varied.

3.1. Turing patterns

Consider a system of nonlinear reaction-diffusion equations in a 3-dimensional domain $\Omega \subseteq \mathbb{R}^3$,

$$\frac{\partial \mathbf{u}}{\partial t} = \mathcal{F}(\mathbf{u}) + D\nabla^2 \mathbf{u}. \tag{2}$$

Here $\mathbf{u} = (u_1, \ldots, u_m) : \Omega \to \mathbb{R}^m$, and $\mathcal{F} = (F_1, \ldots, F_m)$, $m \geq 2$, is a family of sufficiently smooth vector-valued mappings. $D = \operatorname{diag}(d_1, \ldots, d_m)$ is a constant diagonal $m \times m$ matrix, where the diagonal elements d_i are all positive.

Such systems arise in the description of chemicals which diffuse and react with each other. The matrix D contains the diffusion coefficients for each chemical, and the function $\mathcal{F}(\mathbf{u})$ describes the reaction kinetics.

It is an idea dating back to the work of Turing on morphogenesis in the early 1950s that such a system can "generically" exhibit self-organizing behavior and produce spatial patterns [Turing, 1952]. To understand these ideas, we assume that there exists a constant steady state $\mathbf{u}_0$ of system (2), that is, we have $\mathcal{F}(\mathbf{u}_0) = 0$. We assume without any loss of generality that $\mathbf{u}_0 = \mathbf{0} = (0, \ldots, 0)$; this can easily be achieved via a translation of the concentration vector $\mathbf{u}$. Moreover, this steady state is stable with respect to spatially homogeneous pertubations, that is, all the eigenvalues of the linearization matrix $\partial\mathcal{F}/\partial u(\mathbf{0})$ have negative real parts.

Let us denote

$$A = \frac{\partial \mathcal{F}}{\partial \mathbf{u}}(\mathbf{u}_0).$$

Then in the vicinity of $\mathbf{u}_0 = \mathbf{0}$, system (2) can be approximated by the linearized equation

$$\frac{\partial \mathbf{u}}{\partial t} = \left(A + D\nabla^2\right)\mathbf{u}. \tag{3}$$

The solution of the linearized system (3) can be written down quite explicitly. Let k_ν^2 denote the eigenvalues of the operator $-\nabla^2$ on Ω, indexed by $\nu = 0, 1, 2, \ldots$. (These eigenvalues depend on the chosen boundary conditions; note that the corresponding eigenspaces can be of course of dimension 2 or higher.) The solutions of (3) are linear combinations of the form

$$\mathbf{u}(t, x) = \sum_\nu c_\nu e^{\mu_\nu t} W_\nu(x) \cdot \mathbf{v}_\nu, \tag{4}$$

where $\mu_\nu = \mu(k_\nu^2)$ is an eigenvalue of $A - k_\nu^2 D$ with eigenvector $\mathbf{v}_\nu$, and the function $W_\nu(x)$ lies in the eigenspace of k_ν^2. The constants c_ν are determined by a Fourier expansion of the initial conditions in terms of the modes $W_\nu(x) \cdot \mathbf{v}_\nu$. The constant μ_ν is the eigenvalue which determines temporal growth. If the real part of μ_ν is positive, then the corresponding mode $W_\nu(x) \cdot \mathbf{v}_\nu$ will be subject to exponential growth in the linearized equations, and so a spatial pattern corresponding to the mode $W_\nu(x) \cdot \mathbf{v}_\nu$ will form. A necessary condition for the mode $W_\nu(x) \cdot \mathbf{v}_\nu$ to be subject to exponential growth is that the matrix $A - k_\nu^2 D$ has an eigenvalue with positive real part. Let us denote by

$\mu_{max}(k^2)$ the largest eigenvalue of the matrix $A - k^2 D$. For certain configurations of the parameters, there is some interval $K_{max} > k^2 > K_{min}$ where $\mu_{max}(k^2) > 0$, and so a mode (m, n) will be subject to exponential growth if k_ν^2 falls into this interval.

Far from the equilibrium, nonlinear effects in the full equation (2) will typically slow down this growth and the chemical concentrations will form a steady state $\overline{\mathbf{u}}(x)$ which thus satisfies

$$0 = \mathcal{F}(\overline{\mathbf{u}}(x)) + D\nabla^2\overline{\mathbf{u}}(x). \tag{5}$$

Typically, this steady state will resemble the eigenfunction $W_{\nu_i^*}(x)$ which corresponds to the eigenvalue k_ν^2 with the maximum positive growth rate μ_ν. If the interval $[K_{max}, K_{min}]$ of resonant wave numbers is "small", one can deal with the situation analytically using bifurcation analysis. This is done for the cube $[0, \pi]^3$ in [Alber *et al.*, 2005]. In this case, the "resemblance" to the eigenfunctions can be made more precise by noting that this is the first order approximation of $\overline{\mathbf{u}}(x)$ with respect to the bifurcation parameter. That is, if we assume that the Turing bifurcation occurs for the wave number k_*^2, we may write then

$$\overline{\mathbf{u}}(x) = \varepsilon\overline{u} \cdot \mathbf{v}_* + \mathcal{O}(\varepsilon^2), \tag{6}$$

where $\overline{u}(x)$ lies in the eigenspace of the eigenvalue k_*^2, and ε is a small parameter, and $\mathbf{v}_*$ lies in the kernel of the matrix $\frac{\partial \mathcal{F}}{\partial \mathbf{u}}(\mathbf{u}_0) - k_*^2 D$, evaluated at the parameter where the Turing bifurcation occurs. (For more details see Section 4 below.)

If the interval $[K_{max}, K_{min}]$ is large, however, we are in the "far-from equilibrium" range. In this case, the situation can sometimes be analyzed by singular perturbation theory, which treats the case that the diffusion coefficient of the activator d_a tends to zero. While the one-dimensional situation is well-understood, this is presently not the case for dimensions 2 and higher. One known result is that for sufficiently small d_a, the steady state must be unstable [Nishiura and Suzuki, 1998, Nishiura, 2002].

In the following, we aim to investigate the zero level sets of the steady state $\overline{\mathbf{u}}(x)$ defined by (5). We will work with a slightly simpler form.

In the following subsections, we consider a scalar function $\overline{u} \in C^2(\overline{\Omega})$, that satisfies the equation

$$\nabla^2\overline{u}(x) = -\varphi(\overline{u}(x)) \qquad (x \in \Omega \subseteq \mathbb{R}^3), \tag{7}$$

where $\varphi\colon \mathbb{R} \to \mathbb{R}$ is a function of class C^2 with $\varphi(z) = 0$ iff $z = 0$, and $\varphi'(0) \neq 0$.

This assumption is relevant to the study of the Turing patterns $\overline{\mathbf{u}}(x)$ defined by (5) in two ways, namely either as a *first order approximation* close to the Turing bifurcation in the general case, or as the *exact solution* for a certain class of reaction kinetics. More precisely, we have the following two situations:

(i) Assume we are considering the situation close to the Turing bifurcation; suppose the Turing bifurcation occurs for the wave number k_*^2. Choose $\varphi(z) = k_*^2 z$, and let $\overline{u}$ satisfy (7). Then by (6), $\overline{\mathbf{u}}(x) \approx \varepsilon\overline{u}(x)\mathbf{v}_*$ is a first order approximation.

(ii) Consider a special class of reaction kinetics $\mathcal{F}$, namely those that satisfy

$$\mathcal{F}(z \cdot \mathbf{e}) = \varphi(z) D\mathbf{e} \quad \text{for all } z \in \mathbb{R}, \tag{8}$$

where $\mathbf{e} \in \mathbb{R}^m$ is a constant vector. (Note that this assumption restricts the function $\mathcal{F}$ only on the line $\mathbb{R} \cdot \mathbf{e} \subseteq \mathbb{R}^m$. The condition $\varphi(0) = 0$ follows from the general assumptions that $\mathcal{F}(\mathbf{0}) = \mathbf{0}$.)
Make the ansatz $\overline{\mathbf{u}}(x) = \overline{u}(x)\mathbf{e}$. Then (5) reduces to (7).
As an example for a case when the condition (8) is satisfied, consider reaction kinetics of the form

$$\mathcal{F}(u, v) = (\mathbf{A} \cdot (u, v) + P(u, v), \mathbf{B} \cdot (u, v) - P(u, v)),$$

where $\mathbf{A}, \mathbf{B} \in \mathbb{R}^2$ are constant vectors, and P is a polynomial of degree ≥ 2. (The well-known Gray-Scott and Brusselator kinetics are of this type.) Suppose the diffusion matrix is given by $D = \operatorname{diag}(d_1, d_2)$, and let $\mathbf{e} = (1, -d_1/d_2)$. If $\mathbf{e} \cdot (\mathbf{A} + \mathbf{B}) = 0$, then the condition (8) is satisfied with $\varphi(z) = (z\mathbf{A} \cdot \mathbf{e} + P(z, -zd_1/d_2))/d_1$.

Let us finally add an observation on the function φ in general. We could either have $\varphi'(0) > 0$ or $\varphi'(0) < 0$. As we will see in the next section, these two cases are quite different. The following lemma says that certain (very common) boundary conditions force the case $\varphi'(0) > 0$, which is thus the more important one.

Lemma 3.1. *Let $\overline{u}$ be a function that satisfies (7). Suppose $\overline{u} \equiv 0$ on the boundary $\partial\Omega$, or $\frac{\partial \overline{u}}{\partial \mathbf{N}} \equiv 0$ on $\partial\Omega$ (where $\mathbf{N}$ is the normal to the boundary). Then we have $\varphi'(0) > 0$.*

Proof. If we assume the above boundary conditions, we get by Gauss' Divergence Theorem

$$-\int_\Omega \overline{u}\varphi(\overline{u})dx = \int_\Omega \overline{u}\nabla^2\overline{u}dx = -\int_\Omega |\nabla\overline{u}|^2 dx$$

By the assumptions on φ in (7), z and $\varphi(z)$ either have the same sign for any $z \in \mathbb{R}$ (this is the case iff $\varphi'(0) > 0$), or opposite signs (this is the case iff $\varphi'(0) < 0$). By the above equality, $\overline{u}$ and $\varphi(\overline{u})$ have to have the same sign, and so $\varphi'(0) > 0$. □

3.2. Variational principles: Geometric formulation

As in the previous section, let $\overline{u}(x)$ be a function that satisfies (7). We denote the equilibrium concentration level set of $\overline{u}$ by

$$S_0 = \{\overline{u} \equiv 0\} = \{x \in \Omega \colon \overline{u}(x) = 0\}. \tag{9}$$

The set $S_0 \cap \{x \in \Omega \colon |\nabla\overline{u}(x)| > 0\}$ is a regular surface with normal

$$\mathbf{N}_{S_0}(x) = \frac{\nabla\overline{u}}{|\nabla\overline{u}|} \qquad (x \in S_0). \tag{10}$$

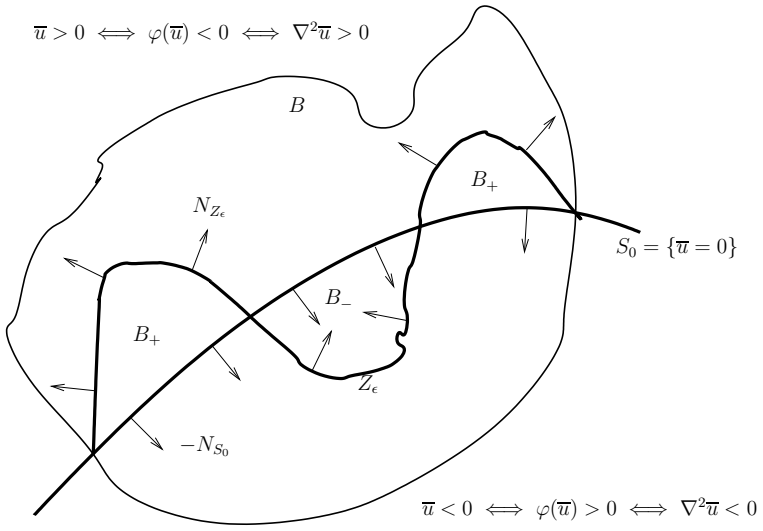

Figure 1. Schematic cross section for the case $\varphi'(0) < 0$. Pictured are the domain B, the zero level surface S_0 and a variation $\mathbf{Z}_\varepsilon$.

In the following, we formulate two variational principle for the surface S_0. For this, we have to formulate a concept of variation of S_0 first. One problem here is that we have to avoid critical points of $\overline{u}$, i.e. points where $\nabla\overline{u} = 0$.

We let $B \subseteq \Omega$ be any open set homeomorphic to a ball with the following properties:

(i) $|\nabla\overline{u}| > 0$ on the closure $\overline{B}$

(ii) $B \setminus S_0$ has exactly two components

(iii) $\partial B \cap S_0$ is a piecewise C^1 curve homeomorphic to the boundary of the unit disk in $\mathbb{R}^2$

Let $D \subseteq \mathbb{R}^2$ be a domain, and let

$$\mathbf{X}\colon \overline{D} \to \overline{B} \subseteq \Omega \subseteq \mathbb{R}^3$$

be a regular parameterization of the zero level set $S_0 \cap \overline{B}$.

In the following, we consider families of surfaces of the form

$$\mathbf{Z}\colon \overline{D} \times (-\varepsilon_0, \varepsilon_0) \to \mathbb{R}^3 \quad (\varepsilon_0 > 0)$$

such that $\mathbf{Z}(\cdot, \varepsilon = 0) = \mathbf{X}$, and $\mathbf{Z}(\cdot, \varepsilon) = S_0 \cap \partial B$ on the boundary ∂B. We will also write $\mathbf{Z}_\varepsilon$ for the surface $\mathbf{Z}(\cdot, \varepsilon)$.

For each ε, the surface $\mathbf{Z}_\varepsilon \cup \mathbf{X}$ is the boundary of two collections of domains B_+ and B_-, where $B_+ \subseteq B \cap \{\overline{u} > 0\}$ and $B_- \subseteq B \cap \{\overline{u} < 0\}$. (See Figure 1.) We choose the orientation of the normal $\mathbf{N}_{\mathbf{Z}_\varepsilon}$ such that the collection $\mathbf{N}_{\mathbf{Z}_\varepsilon} \cup (-\mathbf{N}_{S_0})$ is a normal field for the boundaries of B_+ and B_-. (The normal $\mathbf{N}_{\mathbf{Z}_\varepsilon}$ thus points inwards for B_- and outwards for B_+.)

With these preparations, we can now formulate the following two variational principles:

Theorem 3.2. *(i) Consider the functional*

$$\mathbf{Z}_\varepsilon \mapsto \mathcal{G}_1(\mathbf{Z}_\varepsilon) = \int_{\mathbf{Z}_\varepsilon} \nabla \overline{u} \cdot \mathbf{N}_{\mathbf{Z}_\varepsilon} dS,$$

defined for all surfaces $\mathbf{Z}_\varepsilon$ with normal $\mathbf{N}_{\mathbf{Z}_\varepsilon}$ as constructed in the preceding paragraph.
Then the zero level surface $\mathbf{X} = S_0 \cap B$ minimizes *$\mathcal{G}_1$ if $\varphi'(0) < 0$. The surface $\mathbf{X}$* maximizes *$\mathcal{G}_1$ if $\varphi'(0) > 0$.*

(ii) Consider the functional

$$\mathbf{Z}_\varepsilon \mapsto \mathcal{G}_2(\mathbf{Z}_\varepsilon) = \int_{\mathbf{Z}_\varepsilon} |\nabla \overline{u}| \, dS.$$

We restrict ourselves to surfaces $\mathbf{Z}_\varepsilon$ constructed as in the preceding paragraph such that the projection of $\mathbf{Z}_\varepsilon$ to $\mathbf{X}$ along the normals $\mathbf{N}_\mathbf{X} = \mathbf{N}_{S_0}$ is $1-1$.
Then $\mathbf{X} = S_0 \cap B$ is a critical point of $\mathcal{G}_2$, i.e., for any such family $\mathbf{Z}_\varepsilon$, we have

$$\left.\frac{\partial}{\partial \varepsilon}\right|_{\varepsilon=0} \mathcal{G}_2(\mathbf{Z}_\varepsilon) = 0. \tag{11}$$

Moreover, if $\varphi'(0) < 0$, then $\mathbf{X}$ minimizes $\mathcal{G}_2$.

Proof. **(i)** The proof is an application of Gauss' Divergence Theorem. We will show this for the case $\varphi'(0) < 0$ only. The case $\varphi'(0) > 0$ can be treated analogously with only very slight modifications.

Since $z = 0$ is the only root of $\varphi(z)$, the assumption $\varphi'(0) < 0$ implies that $\varphi(z) > 0$ iff $z < 0$ and $\varphi(z) < 0$ iff $z > 0$. Using (7), one sees that thus $\nabla^2 \overline{u} > 0$ iff $\overline{u} > 0$. Recall the definitions of the domains $B_+ \subseteq B \cap \{\overline{u} > 0\}$ and $B_- \subseteq B \cap \{\overline{u} < 0\}$ on page 10. (The stuation is illustrated in Figure 1.) Using the divergence theorem, we have

$$0 \leq \int_{B_+} \nabla^2 \overline{u} \, dx = \int_{\partial B_+} \nabla \overline{u} \cdot \mathbf{N}_{\partial B_+} dS = \int_{\partial B_+ \cap \mathbf{Z}_\varepsilon} \nabla \overline{u} \cdot \mathbf{N}_{\mathbf{Z}_\varepsilon} \, dS - \int_{\partial B_+ \cap S_0} \nabla \overline{u} \cdot \mathbf{N}_{S_0} \, dS. \tag{12}$$

Likewise, we get

$$0 \geq \int_{B_-} \nabla^2 \overline{u} \, dx = \int_{\partial B_-} \nabla \overline{u} \cdot \mathbf{N}_{\partial B_-} dS = -\int_{\partial B_- \cap \mathbf{Z}_\varepsilon} \nabla \overline{u} \cdot \mathbf{N}_{\mathbf{Z}_\varepsilon} \, dS + \int_{\partial B_- \cap S_0} \nabla \overline{u} \cdot \mathbf{N}_{S_0} \, dS. \tag{13}$$

Subtracting (13) from (12) yields

$$0 \leq \int_{\mathbf{Z}_\varepsilon} \nabla \overline{u} \cdot \mathbf{N}_{\mathbf{Z}_\varepsilon} \, dS - \int_{B \cap S_0} \nabla \overline{u} \cdot \mathbf{N}_{S_0} \, dS = \mathcal{G}_1(\mathbf{Z}_\varepsilon) - \mathcal{G}_1(\mathbf{X}),$$

where we note that of course $B \cap S_0 = \mathbf{X}$. Note that equality holds above if and only if $\mathbf{Z}_\varepsilon = \mathbf{X}$. This establishes the claim.

(ii) We first prove the second claim that $\mathbf{X}$ minimizes $\mathcal{A}_2$ if $\varphi'(0) < 0$. This follows almost immediately from (i). Indeed, we have for any surface $\mathbf{Z}_\varepsilon$,

$$\mathcal{G}_2(\mathbf{X}) = \int_{\mathbf{X}} |\nabla \overline{u}|\, dS = \int_{\mathbf{X}} \nabla \overline{u} \cdot \mathbf{N}_{S_0}\, dS = \mathcal{G}_1(\mathbf{X}) \le \mathcal{G}_1(\mathbf{Z}_\varepsilon) = \int_{\mathbf{Z}_\varepsilon} \nabla \overline{u} \cdot \mathbf{N}_{\mathbf{Z}_\varepsilon}\, dS \le \int_{\mathbf{Z}_\varepsilon} |\nabla \overline{u}|\, dS = \mathcal{G}_2(\mathbf{Z}_\varepsilon),$$

where again we have equality if and only if $\mathbf{Z}_\varepsilon = \mathbf{X}$.

For the case $\varphi'(0) > 0$, the above idea doesn't work, and so we prove the weaker statement (11).

To avoid excessive subscripts, let in the following $\mathbf{N} = \mathbf{N}_{S_0}$ denote the normal of S_0 as defined in (10). By our assumptions, there is a function $h(r, s)$ such that

$$\mathbf{Z}_\varepsilon(r, s) = \mathbf{X}(r, s) + \varepsilon\, h(r, s)\mathbf{N}(r, s) + \mathcal{O}(\varepsilon^2).$$

One computes that the surface area element of $\mathbf{Z}_\varepsilon$ is given by

$$|(\mathbf{Z}_\varepsilon)_r \times (\mathbf{Z}_\varepsilon)_s| = (1 + 2\varepsilon\, h\, H)\, |\mathbf{X}_r \times \mathbf{X}_s| + \mathcal{O}(\varepsilon^2).$$

Here H is the mean curvature of $\mathbf{X}$, and we have used the well-known formula $\mathbf{X}_r \times \mathbf{N}_s + \mathbf{N}_r \times \mathbf{X}_s = 2H\, (\mathbf{X}_r \times \mathbf{X}_s)$.

One also computes the following expansion:

$$\begin{aligned} |\nabla \overline{u}(\mathbf{Z}_\varepsilon)| &= |\nabla \overline{u}(\mathbf{X})| + \varepsilon h \frac{1}{|\nabla \overline{u}(\mathbf{X})|}\, \operatorname{Hess} \overline{u}(\mathbf{X})[N, \nabla \overline{u}(\mathbf{X})] + \mathcal{O}(\varepsilon^2) \\ &= |\nabla \overline{u}(\mathbf{X})| - 2\varepsilon\, h\, H\, |\nabla \overline{u}(\mathbf{X})| + \mathcal{O}(\varepsilon^2). \end{aligned}$$

Here we used the formula (1) for the mean curvature of the level set $\mathbf{X} = S_0 \cap B$; note that $\nabla^2 \overline{u} = 0$ on $\mathbf{X}$ by (7).

With these expansions, we can now compute the first variation of $\mathcal{G}_2$ as follows:

$$\begin{aligned} \mathcal{G}_2(\mathbf{Z}_\varepsilon) &= \int_D |\nabla \overline{u}(\mathbf{Z}_\varepsilon(r, s))|\, |(\mathbf{Z}_\varepsilon)_r \times (\mathbf{Z}_\varepsilon)_s|\, dr\, ds \\ &= \int_D \left(|\nabla \overline{u}(\mathbf{X})| - 2\varepsilon\, h\, H\, |\nabla \overline{u}(\mathbf{X})|\right) (1 + 2\varepsilon\, h\, H)\, |\mathbf{X}_r \times \mathbf{X}_s|)\, dr\, ds + \mathcal{O}(\varepsilon^2) \\ &= \int_D |\nabla \overline{u}(\mathbf{X})|\, |\mathbf{X}_r \times \mathbf{X}_s|\, dr\, ds + \mathcal{O}(\varepsilon^2) = \mathcal{G}_2(\mathbf{X}) + \mathcal{O}(\varepsilon^2). \end{aligned}$$

This proves (11). □

The result of the first part of Theorem 3.2 can be summarized by saying that if we seek a surface through which the diffusive flux of $\overline{u}$ is minimal (for $\varphi'(0) < 0$), or maximal (for $\varphi'(0) > 0$), then the solution is just the equilibrium concentration surface.

Likewise, the result for the case $\varphi'(0) < 0$ in part (i) says that if we seek to minimize the integral $\mathcal{G}_2(S) = \int_S |\nabla \overline{u}|\, dS$ over a surface S, then again, the equilibrium concentration surface is our solution. In the (more important) case $\varphi'(0) > 0$, it is not completely clear whether the level surface is a minimum or saddle point for the

functional $\mathcal{A}_2$, although we strongly expect it to be a saddle point in light of the result of Theorem 3.2(ii).

The extremality of the functional $\mathcal{A}_2$ gives an intuitive argument why the equilibrium concentration surface S_0 can be "close" to an area minimizing surface: Indeed, if we try to minimize the integral $\int_S |\nabla \overline{u}|\, dS$, a good guess would be a surface whose area is as small as possible, in particular if the gradients $\nabla \overline{u}$ do not vary much over the region we are considering. This argumentation can be made quantitative as follows: Suppose we consider a minimal surface S_m and (a part of) the zero level set S_0 that span the same closed curve γ, and such that $\mathrm{Area}(S_m) < \mathrm{Area}(S_0)$, but $\int_{S_m} |\nabla \overline{u}|\, dS > \int_{S_0} |\nabla \overline{u}|\, dS$. Then it is not hard to see that we get the following upper bound for the area difference of S_0 and S_m relative to the area of S_m:

$$\frac{\mathrm{Area}(S_0) - \mathrm{Area}(S_m)}{\mathrm{Area(S_0)}} \leq 1 - \frac{\min_{S_0} |\nabla \overline{u}|}{\max_{S_m} |\nabla \overline{u}|}.$$

Clearly, in the case that the modulus of the gradient $|\nabla \overline{u}|$ is close to constant, one expects a good fit between the minimal surface and the equilibrium concentration surface then.

3.3. Variational principles: Chemical formulation

In the previous subsection, we kept the chemical concentration $\overline{u}(x)$ fixed. We showed that in order to maximize (for $\varphi'(0) > 0$) or to minimize (for $\varphi'(0) < 0$) the gradient flux through a surface S, we should choose the zero level surface S_0. Since we considered variations of this surface, this is a "geometric" result.

In this subsection, we give a "chemical" variational principles, which is essentially a variation of the previous result. Namely, we now consider variations of the chemical concentration $\overline{u}$. As before, let $\overline{u}$ be a function satisfying (7), and let S_0 be its zero level surface. In the following, we prove the analogous statement to Theorem 3.2.

To define variations of $\overline{u}$, let $B \subseteq \Omega$ be an open set as in section 3.2; recall that the main property of B is that we have $|\nabla \overline{u}| > 0$ on $\overline{B}$. In the following, we consider variations of $\overline{u}$ of the form

$$w_\varepsilon(x) = \overline{u}(x) + \varepsilon\, \eta(x) \qquad (x \in B, \varepsilon \in \mathbb{R}), \tag{14}$$

where $\eta(x)$ is a C^2-function with compact support in the open set B, and with the additional orthogonality condition that

$$\nabla \eta \cdot \nabla \overline{u} = 0 \quad \text{on } S_0 \cap B. \tag{15}$$

Theorem 3.3. *Consider the functional $\mathcal{C}$ defined via*

$$w_\varepsilon = \overline{u} + \varepsilon\, \eta \;\mapsto\; \mathcal{C}(w_\varepsilon) = \int_{S_\varepsilon} |\nabla w_\varepsilon|\, dS, \tag{16}$$

where $\eta(x)$ is a function satisfying (15) as defined in the preceding paragraph, and $S_\varepsilon = \{x \in B \colon w_\varepsilon(x) = 0\}$ is the zero level surface of the function w_ε.

Then $\mathcal{C}(w_\varepsilon)$ is well-defined for small enough $|\varepsilon|$, and $\overline{u}$ is a critical point of $\mathcal{C}$. That is, we have

$$\frac{\partial}{\partial\varepsilon}\Big|_{\varepsilon=0} \mathcal{C}(w_\varepsilon) = 0. \tag{17}$$

Proof. Clearly, as $|\nabla\overline{u}| > 0$ on $\overline{B}$, we have $|\nabla w_\varepsilon| > 0$ on $\overline{B}$ if $|\varepsilon|$ is small enough, and so S_ε is a regular surface then. Thus the integral (16) is well-defined if $|\varepsilon|$ is small enough.

We next show that for small enough $|\varepsilon|$, there is a real function $\overline{k}(\varepsilon, x)$ defined for $x \in S_0 \cap B$, such that the map

$$\psi_\varepsilon \colon S_0 \cap B \to S_\varepsilon = \{x \in B \colon w_\varepsilon(x) = 0\}, \quad x \mapsto x + \overline{k}(\varepsilon, x)\, \mathbf{N}_{S_0}(x)$$

is a bijection. (I.e., the projection $S_\varepsilon \to S_0$ along the normals $\mathbf{N}_{S_0}$ is $1-1$. In the following, we will write $\mathbf{N}$ for $\mathbf{N}_{S_0}$ to avoid excessive subscripts.)

In order to construct the function $\overline{k}(\varepsilon, x)$, let $x' \in S_\varepsilon$. Then for $|\varepsilon|$ small enough, there is a unique point $x \in S_0$ and a unique number $\overline{k}(\varepsilon, x)$ such that $x' = x + \overline{k}(\varepsilon, x)\, \mathbf{N}(x)$. This defines implicitly for all small enough $|\varepsilon|$ an assignment $x \mapsto \overline{k}(\varepsilon, x)$, defined for all $x \in S_0$. Note that this assignment $x \mapsto \overline{k}(\varepsilon, x)$ may a priori be a multi map, i.e., the same x can correspond to several numbers $\overline{k}(\varepsilon, x)$ for fixed ε. In order to prove that the map ψ_ε is bijective, we just need to show that the assignment $x \mapsto \overline{k}(\varepsilon, x)$ defines a function on $S_0 \cap B$ for sufficiently small ε (i.e., that every x has a *unique* image $\overline{k}(\varepsilon, x)$).

In order to do so, note first that

$$\frac{\partial}{\partial\lambda}\Big|_{\lambda=0} (\overline{u} + \varepsilon\,\eta)(x + \lambda\, \mathbf{N}(x)) = |\nabla\overline{u}(x)| > 0.$$

(Here we used the condition $\nabla\eta \cdot \nabla\overline{u} = 0$.) So if we choose $\varepsilon_0 > 0$ small enough, we can find a $\delta > 0$ such that

$$\frac{\partial}{\partial\lambda}(\overline{u} + \varepsilon\,\eta)(x + \lambda\, \mathbf{N}(x)) > 0 \quad \text{for all } |\lambda| < \delta, |\varepsilon| < \varepsilon_0.$$

It follows immediately that the equation $(\overline{u} + \varepsilon\,\eta)(x + \lambda\, \mathbf{N}(x)) = 0$ has at most one solution in λ for $|\lambda| < \delta$, $|\varepsilon| < \varepsilon_0$. This solution is of course given by $\lambda = \overline{k}(\varepsilon, x)$, by definition of $\overline{k}(\varepsilon, x)$. One infers that for small enough $|\varepsilon|$, every $x \in S_0 \cap B$ has a *unique* image $\overline{k}(\varepsilon, x)$. This proves that the map ψ_ε is indeed a bijection.

To find the first order approximation of $\overline{k}(\varepsilon, x)$ in ε, we compute

$$0 = \frac{\partial}{\partial\varepsilon}\Big|_{\varepsilon=0} (\overline{u} + \varepsilon\,\eta)(x + \overline{k}(\varepsilon, x)\mathbf{N}) = \eta(x) + |\nabla\overline{u}|\, \frac{\partial}{\partial\varepsilon}\Big|_{\varepsilon=0} \overline{k}(\varepsilon, x),$$

and so $\overline{k}(\varepsilon, x) = -\varepsilon \frac{\eta(x)}{|\nabla\overline{u}(x)|} + \mathcal{O}(\varepsilon^2)$.

So if $\mathbf{X}(r, s)$ is a regular parameterization of $S_0 \cap B$ as in Section 3.2, then

$$\mathbf{Z}_\varepsilon(r, s) = \mathbf{X}(r, s) + \overline{k}(\varepsilon, \mathbf{X}(r, s))\, \mathbf{N}(r, s) = \mathbf{X} - \varepsilon \frac{\eta(\mathbf{X})}{|\nabla\overline{u}(\mathbf{X})|}\mathbf{N} + \mathcal{O}(\varepsilon^2)$$

is a parameterization of the surface $S_\varepsilon = \{w_\varepsilon \equiv 0\}$.

The rest of the proof is carried out a lot like the corresponding part (ii) in Theorem 3.2 with $h(x) = -\varepsilon \frac{\eta(x)}{|\nabla \overline{u}(x)|}$. (See page 12.) The surface element of S_ε is

$$|(\mathbf{Z}_\varepsilon)_r \times (\mathbf{Z}_\varepsilon)_s| = (1 - 2\varepsilon \, \frac{\eta(x)}{|\nabla \overline{u}(x)|} \, H) \, |\mathbf{X}_r \times \mathbf{X}_s| + \mathcal{O}(\varepsilon^2).$$

Furthermore, one computes

$$|\nabla w_\varepsilon(\mathbf{Z}_\varepsilon)| = |\nabla(\overline{u} + \varepsilon \, \eta)(\mathbf{X} - \varepsilon \frac{\eta}{|\nabla \overline{u}|}\mathbf{N} + \mathcal{O}(\varepsilon^2))| = |\nabla \overline{u}(\mathbf{X})| + 2\varepsilon \, \eta H + \mathcal{O}(\varepsilon^2).$$

Here we used again the fact that $\nabla \eta \cdot \nabla \overline{u} = 0$ on $S_0 \cap B$, and the formula (1) for the mean curvature of the level set $S_0 \cap B$.

With these expansions, we can now compute the first variation of $\mathcal{C}$ as follows:

$$\begin{aligned} \mathcal{C}(w_\varepsilon) &= \int_D |\nabla w_\varepsilon(\mathbf{Z}_\varepsilon(r,s))| \, |(\mathbf{Z}_\varepsilon)_r \times (\mathbf{Z}_\varepsilon)_s| \, dr \, ds \\ &= \int_D |\nabla \overline{u}(\mathbf{X})| \, |\mathbf{X}_r \times \mathbf{X}_s| \, dr \, ds + \mathcal{O}(\varepsilon^2) = \mathcal{C}(\overline{u}) + \mathcal{O}(\varepsilon^2). \end{aligned}$$

This proves (17). □

There is again an interesting thermodynamic interpretation of the statement of Theorem 3.3. Recall that in a Turing pattern, the reaction kinetics and diffusion balance each other to produce patterns. If we were able to "turn off" the reaction kinetics, the system would of course equilibrate to the equilibrium concentration $\mathbf{0}$ under the influence of diffusion alone. If a chemical distribution is given by the function $w(x)$, $x \in \Omega$, then the larger the diffusive flux $\int_S \nabla w \cdot N dS$ through a surface S, the faster we reach the equilibrium. The zero level surface $\{w \equiv 0\}$ is of course the interface between the regions of "low" and "high" concentration, and the diffusive flux through it is given by $\int_{\{w \equiv 0\}} \nabla w \cdot N dS = \int_{\{w \equiv 0\}} |\nabla w| dS$ So the variational principle in Theorem 3.3 states, loosely speaking, that the regions of "low" and "high" concentration in Turing patterns are situated in such a way that the diffusive flux from high to low is at a critical value with respect to local variations of the chemical concentration.

4. Patterns close to the Turing Bifurcation in a Box

In this section, we briefly investigate the equilibrium concentration surfaces of patterns close to the Turing bifurcation. Recall the discussion of the emergence of Turing patterns in section 3.1. In this section, we are interested in patterns close to the Turing bifurcation. For this, consider the reaction-diffusion system

$$\frac{\partial \mathbf{u}}{\partial t} = \mathcal{F}(\mathbf{u}, \lambda) + D\nabla^2 \mathbf{u} \tag{18}$$

as in (2), where now the reaction kinetics $\mathcal{F}$ depend on the bifurcation parameter λ. A Turing bifurcation occurs at $\lambda = \lambda_0$ if the constant steady state $\mathbf{u} = \mathbf{0}$ becomes

unstable; i.e. if there is a wave number k_0^2 such that the matrix $\frac{\partial \mathcal{F}}{\partial \mathbf{u}}(0,\lambda) - k^2 D$ has only negative eigenvalues for $\lambda < \lambda_0$ and all $k^2 \geq 0$, but $\frac{\partial \mathcal{F}}{\partial \mathbf{u}}(0, \lambda = \lambda_0) - k_0^2 D$ has a a zero eigenvalue.

In this case, one may introduce a small parameter ε and write the bifurcating branch $\overline{\mathbf{u}}$ and the corresponding bifurcation parameter as

$$\begin{aligned} \overline{\mathbf{u}}_\varepsilon(\mathbf{x}) &= \varepsilon\, u_1(x)\mathbf{v}_0 + \varepsilon^2 \mathbf{u}_2(x) + \cdots \\ \lambda_\varepsilon &= \lambda_0 + \varepsilon\lambda_1 + \cdots . \end{aligned}$$

Here $u_1(x)$ is a solution of the eigenvalue equation $\nabla^2 \overline{u}_1 = -k_0^2 u_1$ with appropriate boundary conditions, and $\mathbf{v_0}$ is a zero eigenvector of the matrix $\frac{\partial \mathcal{F}}{\partial \mathbf{u}}(0, \lambda = \lambda_0) - k_0^2 D$. This standard perturbative technique is carried out e.g. in [Alber *et al.*, 2005], where the stability of 3D Turing patterns with symmetry is investigated.

Consider the special case that the domain Ω is a parallelepiped, $\Omega = [0, L_1] \times [0, L_2] \times [0, L_3]$. We impose *no-flux* (Neumann) conditions on the boundary, i.e. $\partial \overline{\mathbf{u}} / \partial \mathbf{N} = 0$ on $\partial\Omega$, where $\mathbf{N}$ is the normal. Then the solutions of the equation $\nabla^2 \overline{u}_1 = -k_0^2 u_1$ are linear combinations of functions of the form

$$w_{\ell_1,\ell_2,\ell_3}(x,y,z) = \cos\left(\frac{\ell_1 \pi}{L_1} x\right) \cos\left(\frac{\ell_2 \pi}{L_2} y\right) \cos\left(\frac{\ell_3 \pi}{L_3} z\right), \tag{19}$$

where $\ell_1, \ell_2, \ell_3 = 0, 1, 2, \ldots$ are such that

$$\left(\frac{\ell_1 \pi}{L_1}\right)^2 + \left(\frac{\ell_2 \pi}{L_2}\right)^2 + \left(\frac{\ell_3 \pi}{L_3}\right)^2 = k_0^2.$$

"Generically", two of the ℓ's are zero, say $\ell_2 = \ell_3 = 0$ and the corresponding pattern is simply the "sheet" or "lamallae" pattern $\cos(\pi \ell_1 x / L_1)$. If the domain has certain symmetries (more precisely, if the length ratios are rational numbers), there can be other solutions, and in this case, we have several linearly independent functions (19). In this case, the patterns can be more complex.

In the following two subsections, we give two examples for such patterns and show how the equilibrium concentration surfaces of the first order approximation $u_1(x)$ resembles certain minimal surfaces.

4.1. Turing bifurcation in the cube: Nodules versus Lamallae

In this subsection, we follow here the study in [Alber *et al.*, 2005], where the domain is the cube $\Omega = [0, \pi] \times [0, \pi] \times [0, \pi]$ with no-flux boundary conditions, and the wavenumber at which bifurcation occurs is normed to $k_0^2 = 1$. Thus the first order approximations of Turing patterns are given by

$$u_1(x) = s_1 \cos x + s_2 \cos y + s_3 \cos z, \tag{20}$$

where s_1, s_2, s_3 are real parameters. In [Alber *et al.*, 2005], it was shown that there are only three possible cases (up to permutations of x, y, z):

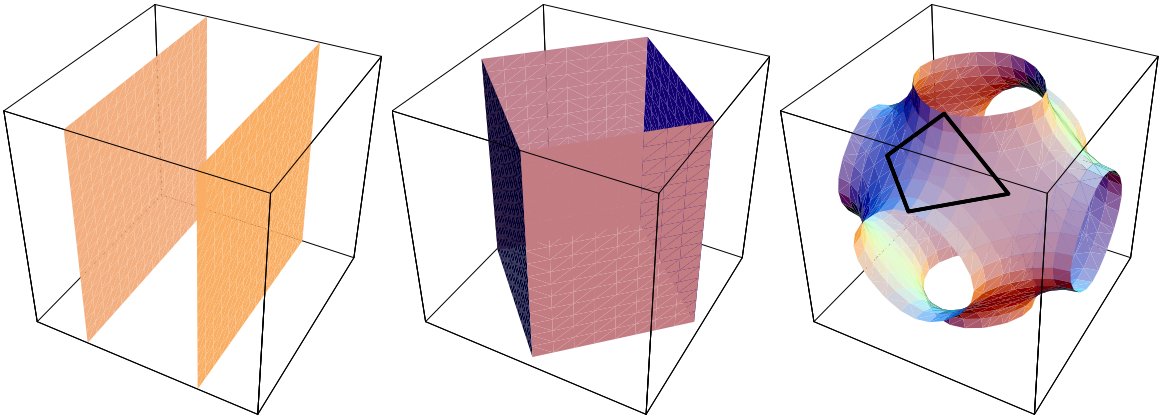

Figure 2. Zero level surfaces of the functions (i) $\cos x$, (ii) $\cos x + \cos y$, and (iii) $\cos x + \cos y + \cos z$ (from left to right) in the cube $[0, 2\pi]^3$. In the third picture, a fundamental domain F_0 bounded by straight line segments is shown. The whole surface can be obtained from reflections of this piece.

(i) $s_1 \neq 0;\ s_2 = s_3 = 0$ (a "sheet" or "lamallae")
(ii) $|s_1| = |s_2| \neq 0;\ s_3 = 0$ (a "cylinder")
(iii) $|s_1| = |s_2| = |s_3| \neq 0$ (a "nodule")

Here we have indicated the shapes of the corresponding patterns. Using bifurcation analysis at a multiple eigenvalue, it was shown that under certain conditions, the cases (i) and (iii) can be linearly stable, but not at the same time. The case (ii) cannot be stable for any set of parameters.

Figure 2 shows plots of the equilibrium surfaces for the function $\cos x$, $\cos x + \cos y$ and $\cos x + \cos y + \cos z$ in the cube $[0, 2\pi]^3$. In the first two cases, these surfaces are simply planes (in the neighborhoods of regular points), and thus in particular locally minimal surfaces.

The interseting case is the case $\cos x + \cos y + \cos z$. The equilibrium concentration has a striking resemblance to Schwarz' P-surface, a triply periodic minimal surface first discovered by R.A. Schwarz in the 1880s. This resemblance has been noted before in a different context in [Lambert *et al.*, 1996]. There, the function $\cos x + \cos y + \cos z$ shows up as the lowest Fourier term of the potential of a collection of point charges whose arrangement in $\mathbb{R}^3$ has the same symmetries as the P-surface. The surface is taken as an approximation of the interface between two domains of a block copolymer. (See the discussion at the end of section 2.2.)

Periodic surfaces resembling the Schwarz P-surface have been reported in cell membranes of a strain of streptomyces, bacteria which resemble fungi in their branching filamentous structure. We hope that our results can be used for the study of three dimensional biological structures, for example biological membranes [Meyer *et al.*, 1990], or skeletal patterns in Echinoidea, where periodic surfaces resembling for instance the Schwarz P-surface have been reported [Pawson and Donnay, 1969, Nissen, 1969].

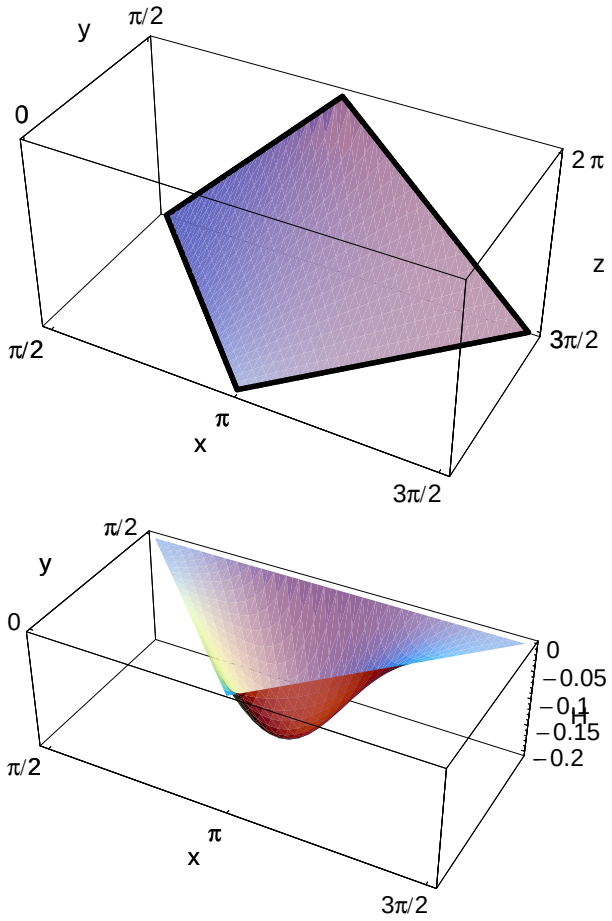

Figure 3. The fundamental surface element from Figure 2 and a plot of its mean curvature as a function of the projection of the surface to the $xy-$plane.

The surface can be obtained by reflections of a fundamental surface element F_0 shown in Figure 2. This surface element is spanned by a skew polygon, i.e. the sides are straight lines. We used K. Brakke's Surface Evolver (see [Brakke, 1992]) to compute the surface area of the minimal surface $F_{\min}$ spanned by this polytope. The difference is given by

$$\frac{\text{Area}(F_0) - \text{Area}(F_{\min})}{\text{Area}(F_{\min})} \approx 0.0028,$$

an amazingly close fit. One computes that the mean curvature at a point (x, y, z) is given by

$$H = \frac{3}{2} \frac{\cos x \cos y \cos z}{(3 - \cos^2 x - \cos^2 y - \cos^2 z)^{3/2}}.$$

Figure 3 shows a plot of the fundamental surface element from Figure 2, along with a plot of its mean curvature. The fact that the mean curvature is close to zero everywhere reflects the good fit to the minimal surface.

4.2. Other examples

The previous subsection treated the case $k_0^2 = 1$ on the cube $[0, \pi]^3$ with no-flux boundary conditions exhaustively, in the sense that we considered all possible bifurcating Turing patterns close to the equilibrium that can arise in this case. In the present subsection, we merely wish to report briefly and without any pretense of depth on an interesting find for more general cases.

Plotting linear combinations of the form (19) for a fixed wave number k^2 suggests that many of these patterns resemble minimal surfaces, especially when the coefficients of the functions (19) have the same modulus, although they often have singular points (i.e., "corners" and self-intersections). An example is plotted in Figure 4 for the function

$$u_1(x, y, z) = \cos(x)\cos(y) + \cos(\sqrt{2}\, z);$$

so $k^2 = 2$. Again, this surface can be constructed from rotations and translations of a fundamental surface element F_1, also pictured in Figure 4. Note that the surface is not regular everywhere, but has a number of "corners". We computed the surface area of the minimal surface that spans the same polytope as the fundamental surface element F_1 using Brakke's Evolver. Here the difference is

$$\frac{\text{Area}(F_1) - \text{Area}(F_{\min})}{\text{Area}(F_{\min})} \approx 0.0130.$$

This is of course merely an example, and we hope to return to a more thorough investigation in a future publication.

5. An analytic explanation for the appearance of Scherk's surface

In the very interesting paper [De Wit *et al.*, 1997], the authors reported on numerical results of Turing structures in the Brusselator reaction-diffusion model. They observed that with the "right" initial conditions, a structure emerged whose equilibrium level surface closely resembled Scherk's surface, a well-known minimal surface. (See Figure 5.) This was verified numerically recently in [Leppänen *et al.*, 2004]. [De Wit *et al.*, 1997] gives a heuristic explanation why certain types of initial conditions should lead to a Scherk-like steady state structure, by making the analogy to the bending of lamellar structures.

The purpose of this section is to give a dynamical explanation of the emergence of "Scherk-like" structures for a certain class of initial conditions by means of linear stability analysis and Fourier analysis. For this, we consider a box

$$\Omega = [0, 2\pi]^2 \times [-\alpha\pi, \alpha\pi], \tag{21}$$

where $\alpha \geq 1$ is some constant. Our results indicate that the appearance of Scherk-like structures can best be observed if the height of the box is roughly equal to the wavelength of the Turing-lamallae. This condition was satisfied in De Wit *et al.* 's numerical example (see [De Wit *et al.*, 1997]).

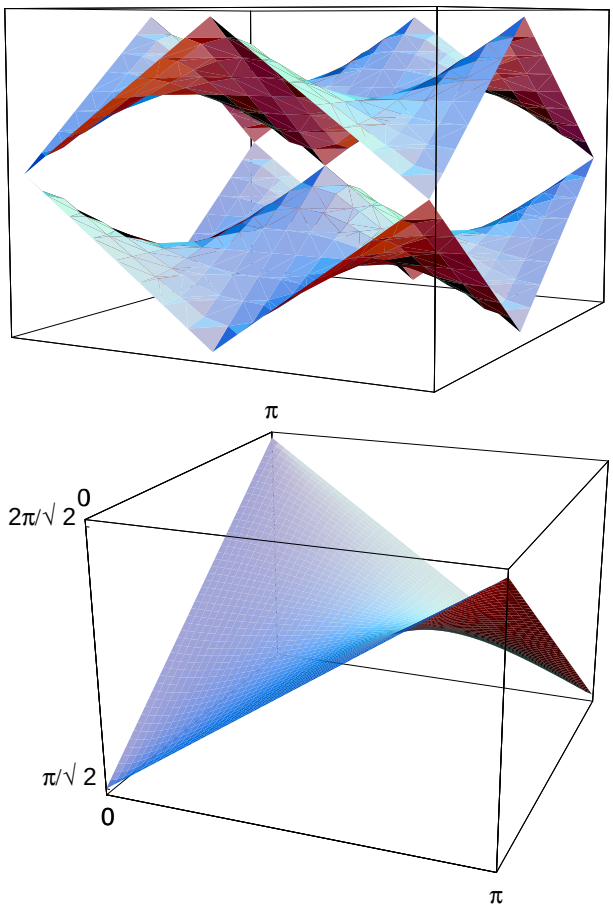

Figure 4. Zero level surfaces of the function $\cos x \cos y + \cos(\sqrt{2}\, z)$ in the rectangle $[0, 2\pi]^2 \times [0, 2\pi/\sqrt{2}]$ (left) and its fundamental surface element.

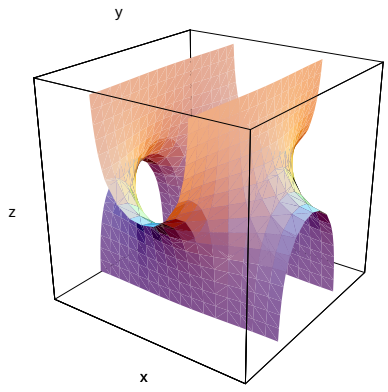

Figure 5. Scherk's first surface, implicitly given by $e^z \cos x = -\cos y$.

The (first) Scherk surface is given implicitly by the equation $e^z \cos x = -\cos y$.† (See Figure 5.) It provides a minimal surface "interpolation" between lamellae perpendicular to the $y-$axis (for $z \to -\infty$) to lamellae perpendicular to the $x-$axis (for $z \to +\infty$). Since both these lamellar structures are possible Turing patterns in the cube by Section 4.1, it is maybe not surprising that with the "right" initial conditions, one gets a Turing pattern which interpolates between the two in the above sense, but what is surely interesting is that this interpolation seems to appear naturally by means of a minimal-surface-like structure. Note that the corresponding pattern is a far-from-equilibrium effect in the sense that it cannot be obtained via the bifurcation analysis of Section 4.1; indeed, it cannot be written as a linear combination of the functions (19).

For our set-up, recall the discussion in Section 3.1. We consider the reaction-diffusion equation (2) with no-flux boundary conditions on the parallelepiped Ω defined as above in (21). We denote again by $A = \frac{\partial \mathcal{F}}{\partial \mathbf{u}}(\mathbf{0})$ the Jacobian of the reaction kinetics at the equilibrium $\mathbf{0}$. An eigenmode with wave vector $\mathbf{k}$ (and corresponding wave number $|\mathbf{k}|^2 = k^2$) is subject to exponential growth in the linearized equation (3) if the dispersion relation

$$(A - k^2 D)\mathbf{v}(k^2) = \mu(k^2)\,\mathbf{v}(k^2) \tag{22}$$

is satisfied for some eigenvector $\mathbf{v}(k)$ with *positive* eigenvalue $\mu(k^2)$. Suppose that the maximum positive eigenvalue $\mu_0^+ > 0$ appears at $k^2 = 1$, and that the other eigenvalue of the matrix $A - D$ is negative. We denote this negative eigenvalue by μ_0^-. Assume we have expansions

$$\begin{aligned}
&\mu^+(k^2) = \mu_0^+ - (k^2-1)^2\bar{\mu} + \mathcal{O}((k^2-1)^3) \qquad (\mu_0^+, \bar{\mu} > 0)\\
&\mu^-(k^2) = \mu_0^- + \mathcal{O}((k^2-1)) \qquad (\mu_0^- < 0)\\
&\mathbf{v}^+(k^2) = \mathbf{v}_0^+ + (k^2-1)\mathbf{v}_1^+ + \mathcal{O}((k^2-1)^2),
\end{aligned}$$

where $\mathbf{v}^+(k^2)$ is the eigenvector for the eigenvalue branch $\mu^+(k^2)$.

Suppose we now set up the initial conditions such that we connect lamellar structures perpendicular to the $y-$axis for $z \approx -\alpha\pi$ to lamellar structures perpendicular to the $x-$axis for $z \approx +\alpha\pi$. For these initial conditions, we thus make the ansatz

$$\mathbf{u}_0(\mathbf{x}) = \mathbf{u}(x, y, z, t = 0) = \frac{\delta}{2}(\cos x + \cos y + \psi(z)\,(\cos x - \cos y))\mathbf{v}_0^+, \tag{23}$$

where $\delta << 1$ is a "small" constant, and $\psi(z)$ is a montone increasing odd function with

$$\psi(-\alpha\pi) = -1,\ \psi(+\alpha\pi) = +1,\ \psi'(-\alpha\pi) = \psi'(+\alpha\pi) = 0.$$

Remark 5.1. Consider the choice $\psi(z) = (\exp z - 1)/(\exp z + 1)$. (This function satisfies the boundary conditions strictly speaking of course only in the limit $\alpha \to \infty$.) Then the zero level set of the initial concentration $\mathbf{u}_0$ is given implicitly via $e^z \cos x = -\cos y$, and so this is Scherk's surface.

† Introducing the shift $y' = y - \pi$, one recovers the more common form $e^z \cos x = \cos y'$ of this equation.

Let $\hat{\psi}(\ell)$ be the ℓth Fourier coefficient of ψ with respect to the basis $\sin((2\ell+1)z/(2\alpha))$ $(\ell = 0, 1, \ldots)$, i.e.

$$\hat{\psi}(\ell) = \frac{1}{\alpha\pi}\int_{-\alpha\pi}^{+\alpha\pi} \psi(z)\sin\left(\frac{(2\ell+1)z}{2\alpha}\right) dz, \qquad \ell = 0, 1, \ldots$$

Note that the first coefficient satisfies $0 \le \hat{\psi}(0) \le \frac{1}{\alpha\pi}\int_{-\alpha\pi}^{+\alpha\pi} \left|\sin(z/2\alpha)\right| dz = 4/\pi$. The case $\hat{\psi}(1) = 4/\pi$ is attained for the discontinuous choice $\psi(z) = z/|z|$.

The solution of the linearized version of the reaction-diffusion equation (18) with initial condition (23) is given by the expansion (4). In our case, this reads

$$\begin{aligned}\mathbf{u}(\mathbf{x},t) =& \frac{\delta}{2}(\cos x + \cos y)e^{\mu_0^+ t}\mathbf{v}_0^+ \\ &+ \frac{\delta}{2}(\cos x - \cos y)e^{\mu_0^+ t}\sum_{\ell=0}^{\infty}\hat{\psi}(\ell)e^{-\varepsilon^4(2\ell+1)^4\bar{\mu}t}\sin\left(\varepsilon(2\ell+1)z\right)(\mathbf{v}_0^+ + \mathcal{O}(\varepsilon^2)) \\ &+ e^{\mu_0^-\, t}G(\mathbf{x},t).\end{aligned}$$

Here we wrote $\varepsilon = 1/2\alpha \le 1/2$, and the remainder $e^{\mu_0^-\, t}G(\mathbf{x},t)$ denotes a term which decays exponentially with time. Because of the factor $e^{\mu_0^+ t}$, we will see the emergence of patterns. If there were no nonlinear terms in (18), the term $(\cos x + \cos y)\mathbf{v}_0^+$ would dominate this pattern in the limit $t \to \infty$. The relative decays of the second and third terms are given by the factors $\varepsilon^{-\varepsilon^4\bar{\mu}t}$ and $\varepsilon^{-81\varepsilon^4\bar{\mu}t}$, respectively. So for shorter times t, the relative decay of the second term is typically still relatively small, whereas decay of the third and higher terms is much faster, so that it is reasonable to approximate the emerging pattern as

$$(\cos x + \cos y)\mathbf{v}_0^+ + (\cos x - \cos y)\hat{\psi}(0)\sin(\varepsilon z)(1-\varepsilon^4\bar{\mu}t)(\mathbf{v}_0^+ + \mathcal{O}(\varepsilon^2)).$$

So the zero level sets are given implicitly via the equation

$$\frac{1 + f(\varepsilon)\hat{\psi}(0)\sin(\varepsilon z)}{1 - f(\varepsilon)\hat{\psi}(0)\sin(\varepsilon z)}\cos x = -\cos y,$$

where $f(\varepsilon) = 1 + \mathcal{O}(\varepsilon^2)$. We compare this level surface with the Scherk surface $e^z\cos x = -\cos y$. If $z >> 0$, we need to have $\cos x \approx 0$, and if $z << 0$, we need to have $\cos y \approx 0$ in both cases. The interesting region is thus $z \approx 0$. We develop the difference of the $z-$dependent functions into a Taylor series at $z = 0$ to get

$$\frac{1 + f(\varepsilon)\hat{\psi}(0)\sin(\varepsilon z)}{1 - f(\varepsilon)\hat{\psi}(0)\sin(\varepsilon z)} - e^z = (-1+2\varepsilon F)z - \frac{1}{2}(1-(2\varepsilon F)^2)z^2 - (\frac{1}{6}+\frac{1}{3}\varepsilon^3 F - 2(\varepsilon F)^3)z^3 + \mathcal{O}(z^4),$$

where $F = F(\varepsilon) = f(\varepsilon)\hat{\psi}(0)$. The above fit is clearly best if $2\varepsilon F = 1$; it is then of the form $-\frac{1}{12}(1 - 1/2F^2)z^3 + \mathcal{O}(z^4)$. Recall that $0 \le \hat{\psi}(0) \le 4/\pi$, where the maximum is attained for $\psi(z) = z/|z|$. If the derivative $\psi'(0)$ is sufficiently steep, we get $\hat{\psi}(0) \approx 1$. Noting that $\varepsilon = 1/2\alpha$, we get best fit of the zero level surface to Scherk's surface for

$$\alpha \approx 1.$$

(This is to be taken as a rough estimate because our previous argumentation relied of course on $\varepsilon = 1/2\alpha$ being "small".) Nevertheless the argumentation gives a clear idea that the fit to Scherk's surface ought to be best if the width of the box is approximately equal to the wavelength of the Turing pattern.

Of course it is not possible with linear analysis to show rigorously that a "Scherk-like" structure is a possible Turing pattern in this situation, but the above argument supports the existence of the numerically obtained results in [De Wit *et al.*, 1997] and [Leppänen *et al.*, 2004]. It would be interesting to get a rigorous construction of this pattern.

Alber, M., Glimm, T., Hentschel, H., Kazmierczak, B. and Newman, S. [2005] "Stability of n–dimensional patterns in a generalized Turing system: implications for biological pattern formation," *Nonlinearity* **18**, 125–138.

Brakke, K. A. [1992] "The surface evolver," *Experiment. Math.* **1**(2), 141–165.

Callahan, T. K. and Knobloch, E. [1997] "Symmetry-breaking bifurcations on cubic lattices," *Nonlinearity* **10**(5), 1179–1216.

Callahan, T. K. and Knobloch, E. [1999] "Pattern formation in three-dimensional reaction-diffusion systems," *Phys. D* **132**(3), 339–362.

Castets, V., Dulos, E., Boissonade, J. and DeKepper, P. [1990] "Experimental evidence of a sustained standing Turing-type nonequilibrium chemical pattern," *Phys. Rev. Lett.* **64**, 2953–2956.

De Wit, A., Borckmans, P. and Dewel, G. [1997] "Twist grain boundaries in three-dimensional lamellar Turing structures," *Proc. Natl. Acad. Sci. USA* **94**, 12765–12768.

Dierkes, U., Hildebrandt, S., Küster, A. and Wohlrab, O. [1992] *Minimal surfaces. I and II*, Vol. 295 and 296 of *Grundlehren der Mathematischen Wissenschaften [Fundamental Principles of Mathematical Sciences]*, Springer-Verlag, Berlin.

Hentschel, H. G. E., Glimm, T., Glazier, J. A. and Newman, S. A. [2004] "Dynamical mechanisms for skeletal pattern formation in the vertebrate limb," *Proc R Soc Lond B Biol Sci* **271**(1549), 1713–1722.

Hoffman, D. [1996] "Mixing mathematics and materials," *MSRI Preprint* (1996-078).
`http://www.msri.org/publications/sgp/david/papers/nature96/`

Izaguirre, J. A., Chaturvedi, R., Huang, C., Cickovski, T., Coffland, J., Thomas, G., Forgacs, G., Alber, M., Hentschel, G., Newman, S. A. and Glazier, J. A. [2004] "CompuCell, a multi-model framework for simulation of morphogenesis," *Bioinformatics* **20**(7), 1129–1137. Evaluation Studies.

Lambert, C., Radzilowski, L. and Thomas, E. [1996] "Triply periodic level surfaces as models for cubic tricontinuous block copolymer morphologies," *Phil. Trans. R. Soc. Lond. A* **354**(1891), 2009–2023.

Leppänen, T., Karttunen, M., Barrio, R. and Kaski, K. [2004] "Turing systems as models of complex pattern formation," *Brazilian Journal of Physics* **34**(2A), 368–372.

Meyer, H. W., Richter, W. and Gumpert, J. [1990] "Periodically curved bilayer structures observed in hyphal cells or stable L-form cells of a Streptomyces strain, and in liposomes formed by the extracted lipids," *Biochim Biophys Acta* **1026**(2), 171–178.

Miura, T. and Maini, P. K. [2004] "Speed of pattern appearance in reaction-diffusion models: implications in the pattern formation of limb bud mesenchyme cells," *Bull Math Biol* **66**(4), 627–649.

Murray, J. D. [2002] *Mathematical biology. I*, Vol. 17 of *Interdisciplinary Applied Mathematics*, third edn, Springer-Verlag, New York.

Newman, S. A. and Frisch, H. L. [1979] "Dynamics of skeletal pattern formation in developing chick limb," *Science* **205**(4407), 662–668.

Nishiura, Y. [2002] *Far-from-equilibrium dynamics*, Vol. 209 of *Translations of Mathematical Monographs*, American Mathematical Society, Providence, RI. Translated from the 1999 Japanese original by Kunimochi Sakamoto, Iwanami Series in Modern Mathematics.

Nishiura, Y. and Suzuki, H. [1998] "Nonexistence of higher-dimensional stable Turing patterns in the singular limit," *SIAM J. Math. Anal.* **29**(5), 1087–1105 (electronic).

Nissen, H.-U. [1969] "Crystal orientation and plate structure in echinoid skeletal units," *Science* **166**, 1150–1152.

Nitsche, J. C. C. [1989] *Lectures on minimal surfaces. Vol. 1*, Cambridge University Press, Cambridge.

Osserman, R. [1986] *A survey of minimal surfaces*, second edn, Dover Publications Inc., New York.

Ouyang, Q. and Swinney, H. [1991] "Transition from a uniform state to hexagonal and striped Turing patterns," *Nature* **352**, 610–612.

Pawson, D. and Donnay, G. [1969] "X-ray diffraction study of echinoderm plates," *Science* **166**, 1147–1150.

Ros, A. [2005] The isoperimetric problem, *in* "Global theory of minimal surfaces," Vol. 2 of *Clay Math. Proc.*, Amer. Math. Soc., Providence, RI, pp. 175–209.

Shoji, H., Iwasa, Y., Mochizuki, A. and Kondo, S. [2002] "Directionality of stripes formed by anisotropic reaction-diffusion models," *J Theor Biol* **214**(4), 549–561.

Thomas, E. L. [1999] "MATERIALS SCIENCE: Enhanced: The ABCs of Self-Assembly," *Science* **286**(5443), 1307.
`http://www.sciencemag.org`

Torquato, S., Hyun, S. and Donev, A. [2002] "Multifunctional composites: optimizing microstructures for simultaneous transport of heat and electricity," *Phys Rev Lett* **89**(26), 266601.

Turing, A. M. [1952] "The chemical basis of morphogenesis," *Philosophical Transactions of the Royal Society (B)* **237**, 37–72.